Phenomenology of Heavy Quarks with Nucleus

M. B. Gay Ducati

beatriz.gay@ufrgs.br

High Energy Particle Phenomenology Group - GFPAE
Universidade Federal do Rio Grande do Sul
Porto Alegre, Brazil

QNP 2015, Valparaiso
2-6/March/2015

Outline

- Motivation
- Nuclear Effects
- EMC
- Quarkonium production
  - Leptoproduction of J/ψ
  - Vector meson dominance
  - Hadroproduction of J/ψ
- Initial state effects
- J/ψ suppression
- Evolution in QCD
  - Saturation
  - Non-linear Effects
  - Diffraction
  - RHIC X LHC - p_T dependence
- Next

Motivation

- In high energy collisions with nucleus, nuclear effects should be considered in order to obtain reliable results.
  - The conventional method for the study of these effects is related to the analysis of quark distribution.
  - However, in accelerators like RHIC and LHC, kinematic regions of small x can be reached where the distribution of gluons is dominant.
  - One way to obtain this distribution is by analyzing the production of heavy quarks states (quarkonium).
  - Quarkonium production involves two steps: one perturbative and a non-perturbative.

Motivation

- The large mass of heavy quarks, allows perturbative QCD calculations, even including non-linear terms.
  - Comparison with the data, should indicate effects from the non-perturbative region.
  - It can also contribute to the investigation of the plasma of quarks and gluons (QGP) in nuclear collisions at high energy.
  - Still, to obtain further clarification on the structure of the Pomeron through hard diffractive scattering involving heavy quarks.

Nuclear Effects

- In proton-nucleus collisions (pA) or nucleus-nucleus (AA),

$$F_2^A\left(x, Q^2\right) \neq A F_2^n\left(x, Q^2\right)$$

- This is due to the *nuclear effects*:
  - Cold matter effects: shadowing effects, nuclear absorption, energy loss in the cold nuclear medium, etc.
  - Hot matter effects: energy loss in the quark gluon plasma (QGP), etc.

Nuclear effects

- In order to estimate the size of these effects, the ratio is defined

$$R_{F_2}^A = \frac{F_2^A\left(x, Q^2\right)}{AF_2^n\left(x, Q^2\right)},$$

more accurately, should include the number of participants

$$R_{AB}(b) = \frac{\frac{dN^{AB}}{dy}(b)}{N_{coll}(b)\frac{dN^{pp}}{dy}}$$

Nuclear Effects

The nuclear shadowing effects can be divided into:

- Shadowing e Anti-shadowing
  - The first features a suppression effect, $R^A_{F_2} < 1$, covering the kinematical region of $x < 0.05$.
  - While the second presents an enhancement effect, $R^A_{F_2} > 1$, acting in the kinematic region of $0.05 - 0.1 < x < 0.2$.
- EMC
  - Suppression effect in the region $0.2 < x < 0.8$, with minimum value near $x \approx 0.65$
- Fermi motion
  - Effect more visible in low energy region $\sqrt{s} \lesssim 50$ GeV.

    A. Szczurek and A. Budzanowski, Mod. Phys. Lett. **A 19** (2004) 1669.
  - However, it is relevant in the forward production study ($\eta \approx 1$), both at RHIC as LHC.

Nuclear Shadowing Effects

- The universal dependence on x for nuclear shadowing effects:

hadr

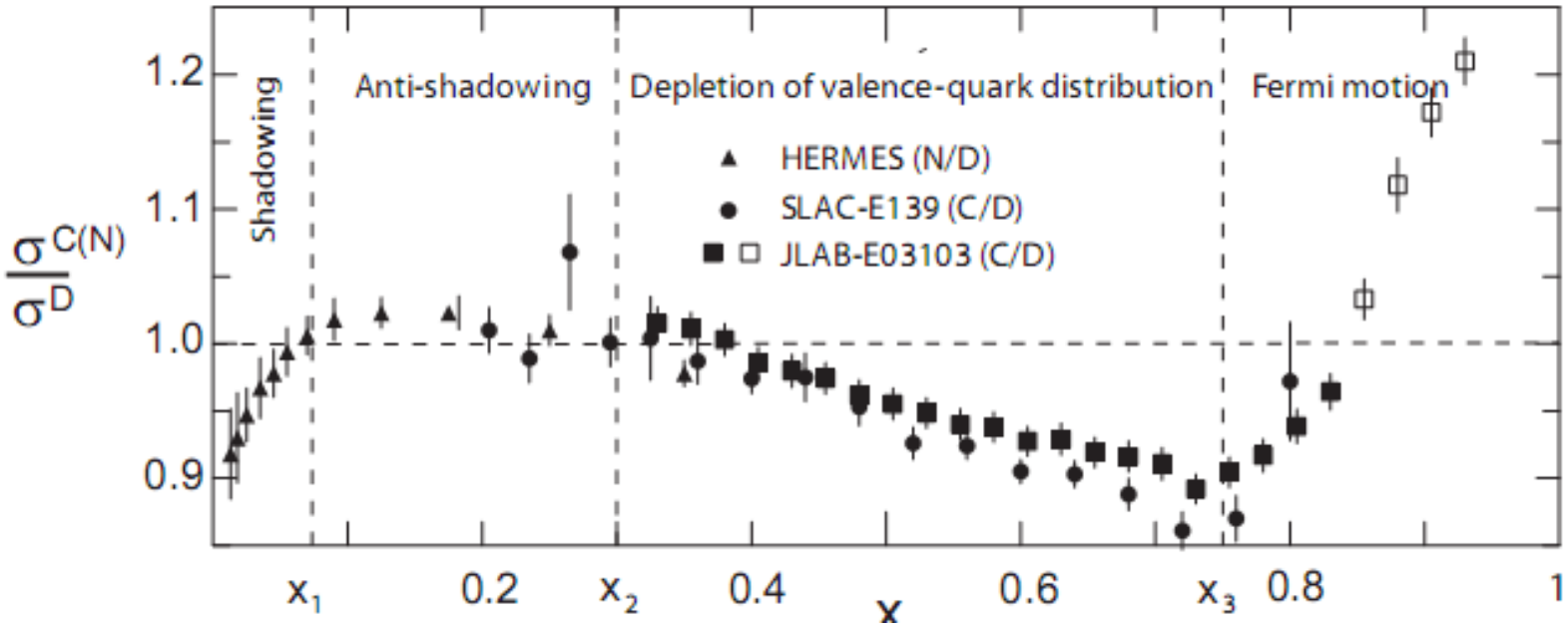

The ratio $\sigma^{C(N)}/\sigma^{D}$ as a function of x from HERMES A. Airapetian et al. (HERMES), Phys. Lett. **B 567** (2003) 339, SLAC-E139 J. Gomez et al. (SLAC-E139), Phys. Rev. **D 49** (1994) 4348, and JLAB-E03103 J. Seely et al. (JLAB-E03103), Phys. Rev. Lett. **103** (2009) 202301. Open squares denote W^2 below 2 GeV^2, where W is the invariant mass of the photon-nucleon system K. Rith, hep-ex 1402.5000.

Other Effects

- Other types of nuclear effects include:
  - Nuclear absorption;
  - Energy loss in the cold nuclear medium;
  - Energy loss in the QGP;
  - Short range correlations;
  - ...

Nuclear Effect EMC

- EMC effect, in particular, was completely unexpected.
- Expected predictions very different of the data.

J.J. Albert et al. (EMC), Phys. Lett. **B 123** (1983) 275

- Nuclear binding effects $\rightarrow$ MeV.
- Probe $\rightarrow$ GeV.

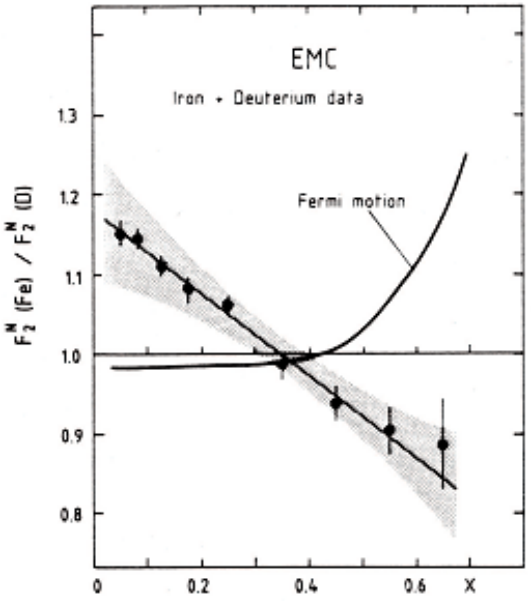

The ratio $F_2^{Fe}/F_2^D(\sigma^{Fe}/\sigma^D)$ as a function of x.

Nuclear Effect EMC

- New data contributed in the formulation of some assumption:
  - Scaling with the atomic mass A, with minimal near $x \approx 0.7$.
  - Linear dependence with the average nuclear density.

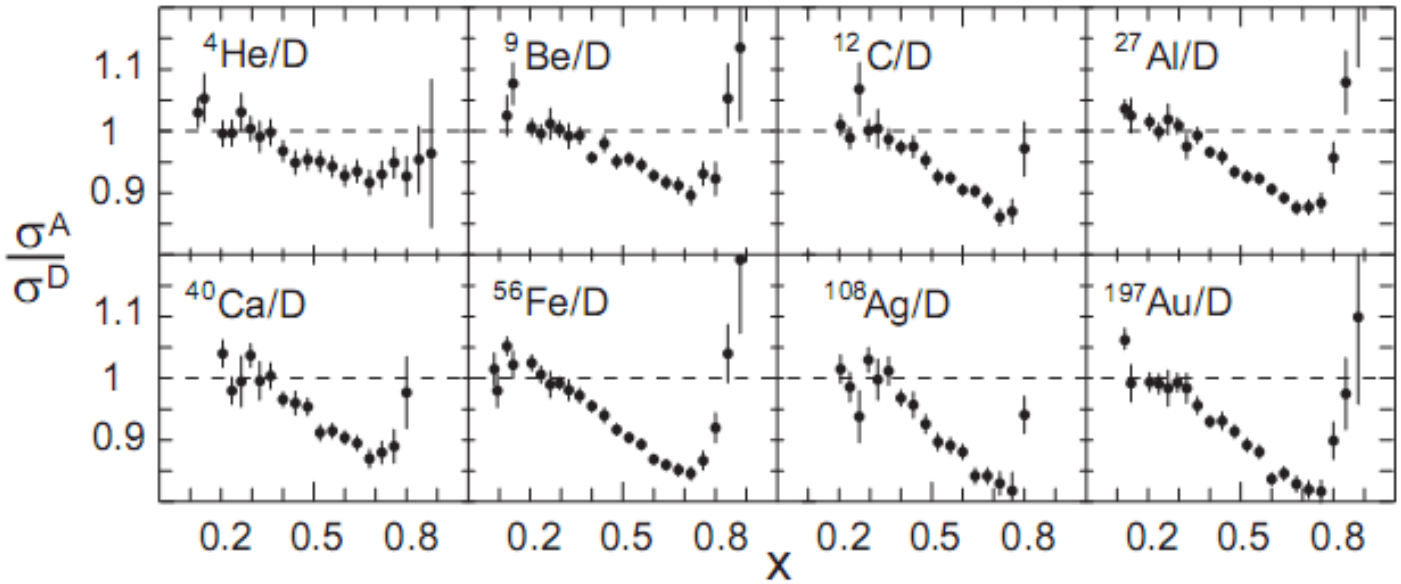

The ratio σ^A/σ^D as a function of x for various nuclei measured by SLAC-E139 R. G. Arnold et al. (SLAC-E139), Phys. Rev. Lett. **52** (1984) 727; J. Gomez et al. (SLAC-E139), Phys. Rev. **D 49** (1994) 4348

Nuclear Effect EMC

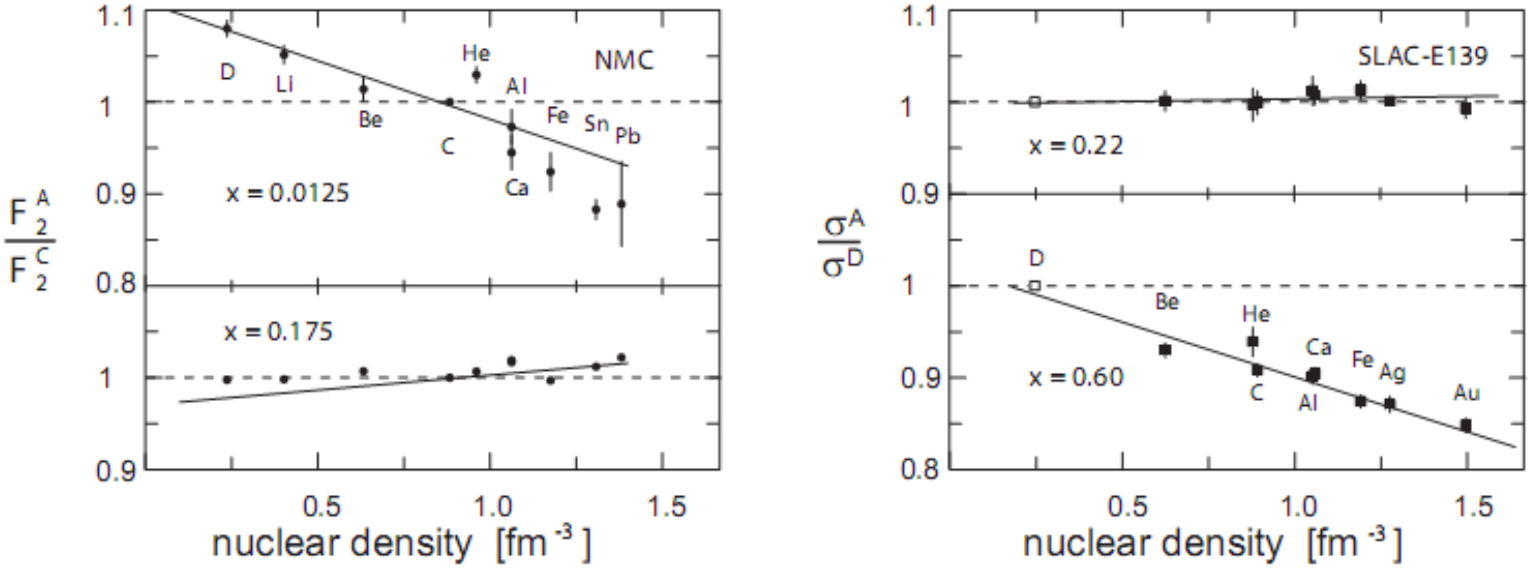

F_2^A/F_2^C as a function of nuclear density ρ at low x from NMC M. Arneodo et al. (NMC), Nucl. Phys. **B 481** (1996) 3 and σ^A/σ^D at high x from SLAC-E139 J. Gomez et al. (SLAC-E139), Phys. Rev. **D 49** (1994) 4348

First Approach

- The study of nuclear effects was based on the analysis of the distribution of quark and antiquarks in the nuclei.
  - Only one indirect distribution can be obtained by the DIS process.
  - Quarks and gluons are closely coupled and it is natural to expect also a change in the distribution of gluons.
  - In the current colliders, RHIC and LHC, the energy is high enough for the gluons distribuition domination.
  - More direct information on this distribution can be achieved by producing states as charmonium or bottomonium.

Quarkonium Production

- Quarkonium is considered any bound state $Q\bar{Q}$ of heavy quarks - charmonium ($c\bar{c}$) or bottomonium ($b\bar{b}$).
- The production of heavy resonances occurs in two steps:
  - The production of heavy quark-antiquark pairs (perturbative).
  - Their resonance interactions to form the bound state (non-perturbative).
- Due to the large mass of quarks involved in the production of quarkonium we can get more reliable information on the scale of short distances via perturbative QCD.

Charmonium Production

- Can shied light on
  - Role of non-perturbative aspects of QCD.
  - Additional study of gluon distribution in the nuclei (although model dependent).
  - Better understanding of the pomeron structure.
  - Opportunity to obtain more precise information about the QGP.

Leptoproduction of J/ψ

- The virtual photoproduction of J/ψ allows us to obtain cleaner information of the hard processes in QCD.
- The theoretical models of these processes can be separated into:
  - Photon-Gluon Fusion Model: it is dominant in the photoproduction of J/ψ.
  - Vector Meson Dominance Models: usually applied in the diffractive photoproduction of J/ψ.
  - Quark-Antiquark Fusion Model,

Photon-Gluon Fusion

- It is the dominant process in the leptoproduction (or photoproduction) of J/ψ: $\gamma + g_1 \to J/\psi + g_2$
- This allows to obtain direct information about the gluon distribuition in the nucleon.

- In the process $\gamma N \to c\bar{c}$, using factorization, $\gamma g \to c\bar{c}$ cross sections combined with the distribution of gluons $G(x, Q^2)$ of the nucleon.

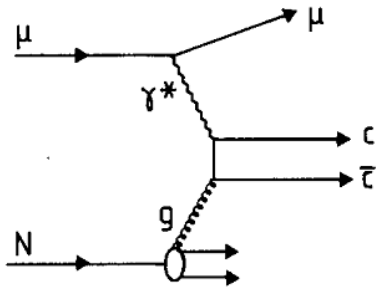

The photon-gluon fusion process for J/ψ photoproduction J.J. Aubert et al. (EMC), Nucl. Phys. **B 213** (1983) 1

Vector Meson Dominance

- This process is also useful in studying the distribution of gluons.

  M. G. Ryskin et al, Z. Phys. **C 76** (1997) 231; D. Kharzeev D et al, Eur. J. Phys. **C 9** (1999) 459.

- The diffractive photoproduction of J/ψ is dominated by vector meson dominance model, J. J. Sakurai and D. Schildknecht, Phys. Lett. **40 B** (1972) 121; T. Bauer et al, Rev. Mod. Phys. **50** (1978) 261.

- The photon is coupled with the J/ψ, that emerges like a hadron.

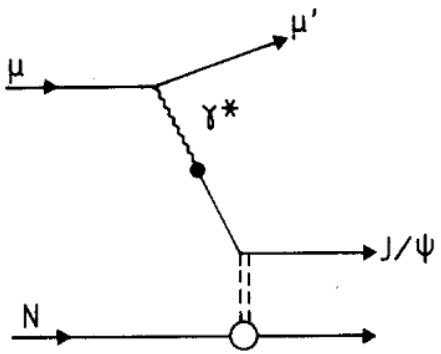

The vector meson dominance model for J/ψ production J.J. Aubert et al. (EMC), Nucl. Phys. **B 213** (1983) 1

Hadroproduction of J/ψ

- The main contributions to the direct hadroproduction of J/ψ in leading order come from: $q\bar{q} \to c\bar{c}$ e $gg \to c\bar{c}$.

  C.A. Garcia Canal, M.B. Gay Ducati, E.M. Santangelo, Phys. Rev. **D 31** (1985) 2748.

- But it is already known that next leading order contributions are very relevant.

  P. Nason, S. Dawson and R.K. Ellis, Nucl. Phys. **B 303**, (1988) 607; **B 327**, (1988) 49.

  M.L. Mangano, P. Nason, G. Ridol, Nucl. Phys. **B 373**, (1992) 295.

- The hadroproduction of J/ψ is useful in the study of gluon distribution in the nucleon in the small-x region.

  L.N. Epele, C.A. Garcia Canal, M.B. Gay Ducati, Phys. Lett. **B 226** (1989) 167.

- This process is also useful in the investigation of suppression J/ψ in the QGP.

  T. Matsui and H. Satz, Phys. Lett. **B 178** (1986) 151

Hadroproduction of J/ψ

- Non-perturbative aspects of this production are included in:
  - Colour Singlet Model (CSM)
  - Colour Evaporation Model (CEM)
  - Soft Colour Interaction model (SCI)
  - Colour Octet Model (COM)

Colour Singlet Model

- Only colorless process.
- Quantum number of the meson equal those of the partonic $c\bar{c}$ pair
- Unable to describe the data Tevatron $\rightarrow$ prediction of up to 50 times lower to ψ'.

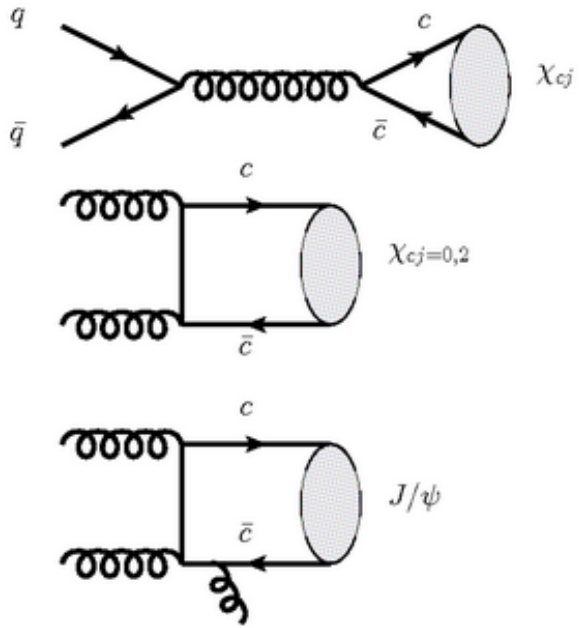

Diagrams considered in CSM.

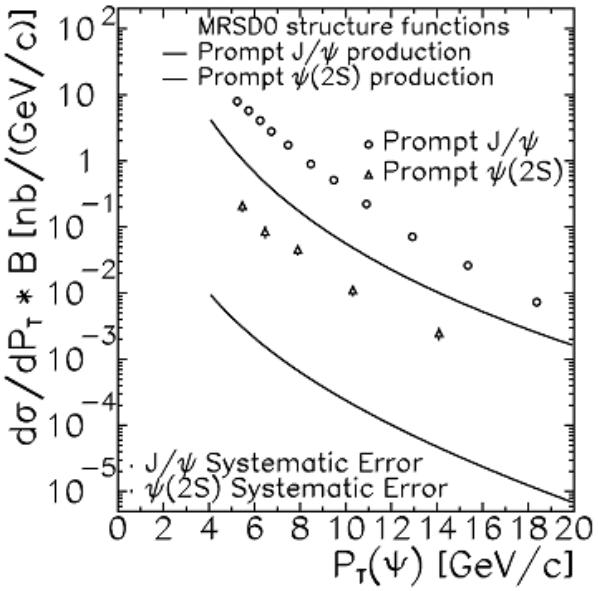

The differential cross section times branching ratio $\mathcal{B}\left(\psi \rightarrow \mu^+\mu^-\right)$ for $\left|\eta^\psi\right| < 0.6$ for prompt ψ mesons. Circles: J/ψ; triangles: $\psi(2S)$ F. Abe et al. Phys. Rev. Lett. **79**, (1997) 572

Colour Evaporation Model

- This model assumes the probability of 1/9 of the state $c\bar{c}$ become colour singlet after numerous exchanges of soft gluons with debris of the reaction.
  - Subsequently, the states with mass below the open charm production threshold produce the charmonium.

$$\sigma_{\text{charmonium}} = \frac{1}{9}\int_{2m_c}^{2m_D} dm_{c\bar{c}}\,\frac{d\sigma_{c\bar{c}}}{dm_{c\bar{c}}}$$

  - The colour octet $c\bar{c}$ states plus the state above that threshold produce open charm.
  - The cross-section is then given by:

$$\sigma_{\text{open}} = \frac{8}{9}\int_{2m_c}^{2m_D} dm_{c\bar{c}}\,\frac{d\sigma_{c\bar{c}}}{dm_{c\bar{c}}} + \int_{2m_D}^{\sqrt{s}} dm_{c\bar{c}}\,\frac{d\sigma_{c\bar{c}}}{dm_{c\bar{c}}}$$

Colour Evaporation Model

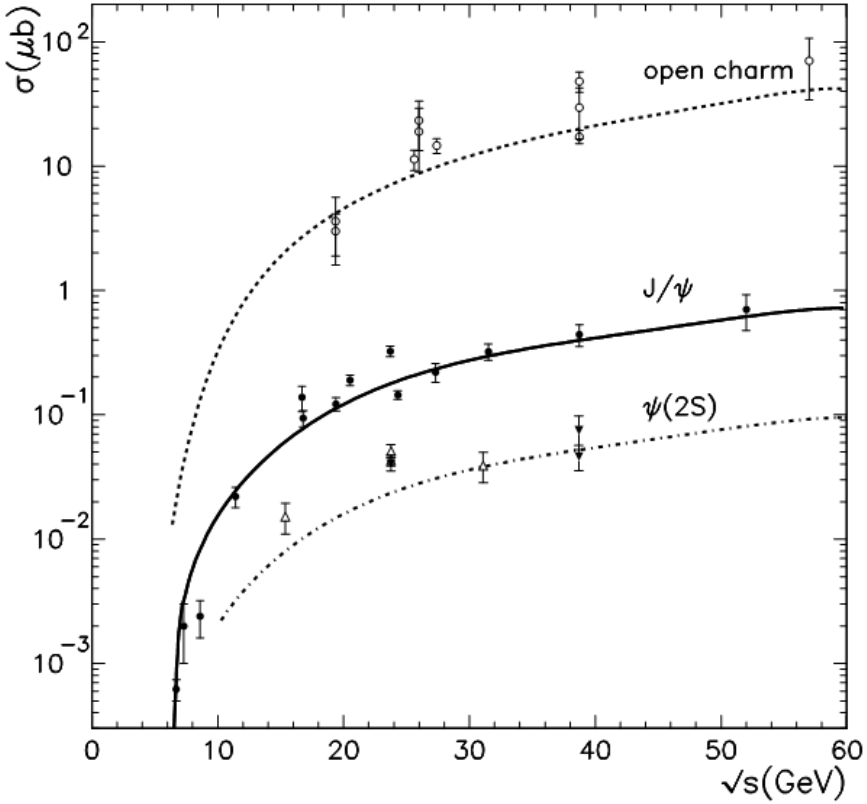

Total cross section of J/ψ, $\psi^{'}$ and open charm (D mesons) in proton-proton interactions at invariant mass $\sqrt{s}$; curves otained from the CEM-NLO model (color evaporation model combined with NLO pQCD matrix elements) in comparison to a compilation of data, C. B. Mariotto, M. B. Gay Ducati, G. Ingelman, Eur.Phys.J. **C 23** (2002) 527 and experimental references therein.

Colour Evaporation Model

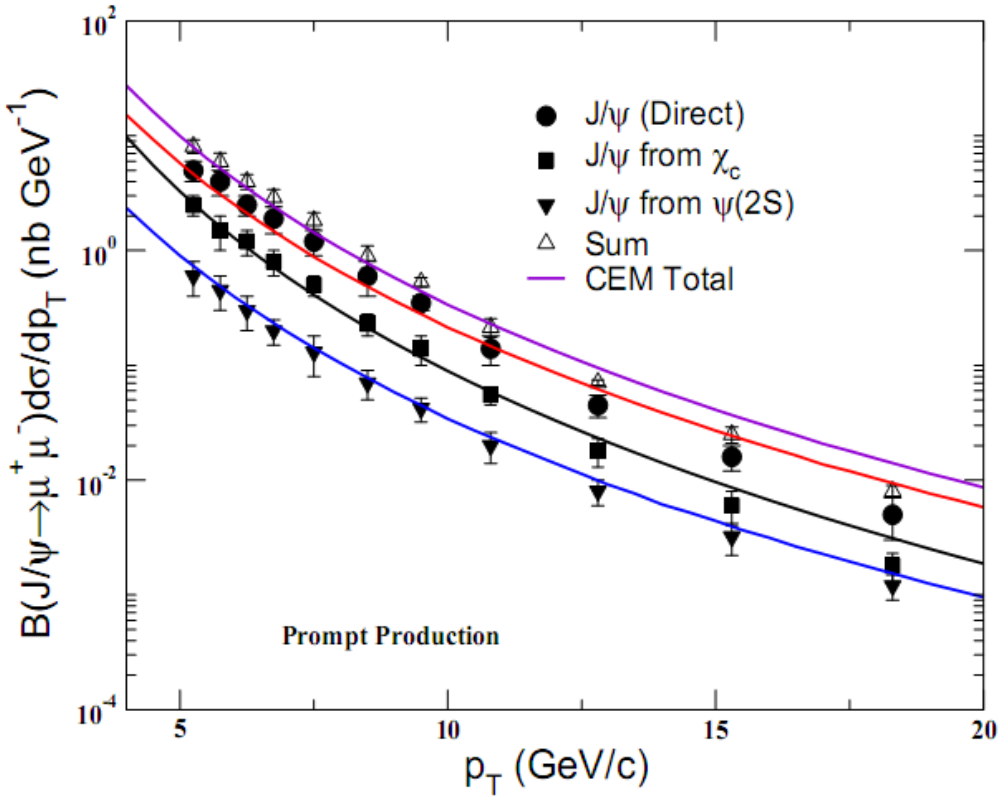

CDF data for prompt J/ψ production is compared with CEM (LO plus gluon splitting) prediction at $\sqrt{s}$=1800 GeV. CTEQ (LO) has been used in all the calculations, P. Roy, A. K. Dutt-Mazumder, Jan-e Alam, nucl-th/0504076 and experimental references therein.

Soft Colour Singlet model

- Monte Carlo model originally proposed to analyze the gaps in rapidity for DIS.

  A. Edin, G. Ingelman, J. Rathsman, Phys. Rev. **D 56** (1997) 7317.

- A phenomenological parameter R is included to quantify the probability of interaction between the partons and the debris of the reaction.
- The pair mapping $c\bar{c}$, below the open charms production threshold, is done by statistical spin.
- This results in a fraction of a specific state of quarkonium i with total momentum angular J_i, given by

$$f_i = \frac{\Gamma_i}{\sum_k \Gamma_k}$$

where $\Gamma(2J_i + 1)/n_i$ corresponds to a partial width.

Colour Octet Model

- $Q\bar{Q}$ pair emits a long wavelenght gluon far away from the collision point.
- Described in NRQCD framework.

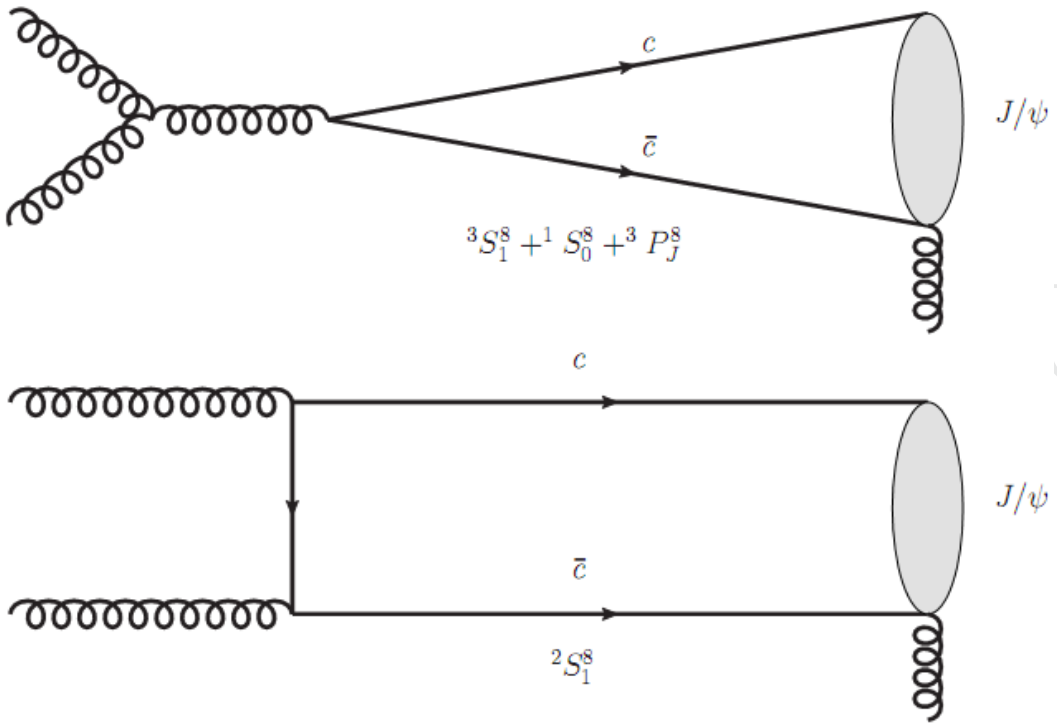

Colour Octet Model

- Direct J/ψ produced.

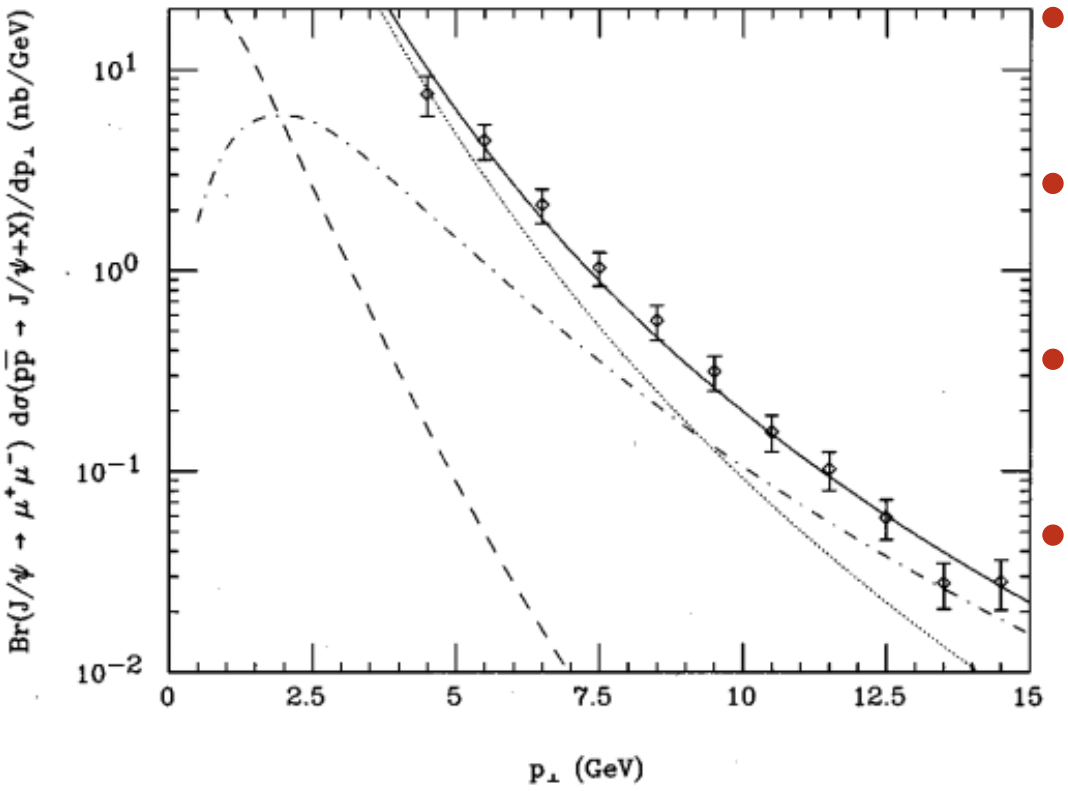

- Dashed curves: direct color-singlet production predictions.
- Dot-dashed: best fits for the $c\bar{c}\left[{}^3S_1^{(8)}\right]$.
- Dotted: combined $c\bar{c}\left[{}^3P_J^{(8)}\right]$ plus $c\bar{c}\left[{}^1S_0^{(8)}\right]$ channels.
- Solid: sums of the color-singlet and color-octet components

P. Cho and A. K. Leibovich, Phys. Rev. **D 53** (1996) 6203

Initial Effects State in Low-x

- Included effective J/ψ absortion.

  L.N. Epele, C.A. Garcia Canal, M.B. Gay Ducati, Phys. Lett. **B 226** (1989) 167

- $\pi A \to J/\psi$ process.
- Nuclear effects $\to R_A(x, Q_0^2, A) = R_{ss}(x_2) R_s(x, Q_0^2, A) R_a(x, Q_0^2, A)$

where

- $R_{ss} \to$ additional nuclear effect.
- $R_s \to$ shadowing by low density parton recombination.
- $R_a \to$ ratio for standard EMC effects.

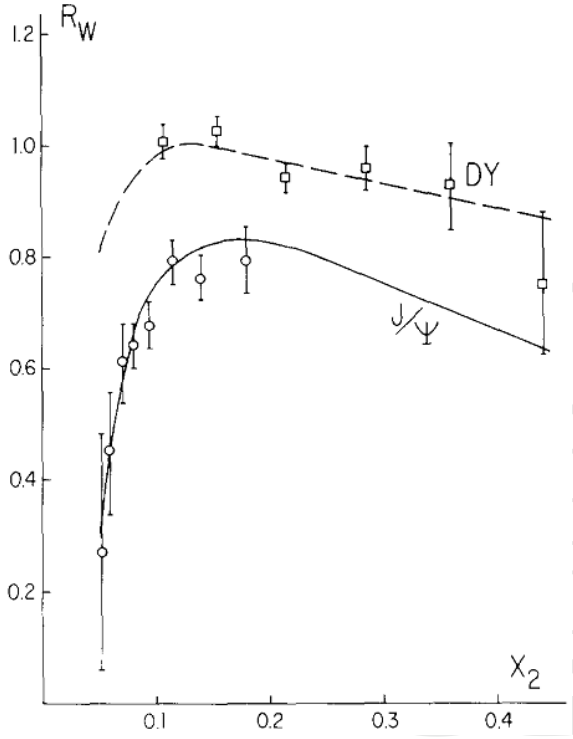

Prediction of the shadowing model of E.L. Berger and J. Qiu, ANL-HEP-CP 88-42-1989 for the ratio R_W^{DY} (dashed curve), and our prediction including absorption effects for the ratio $R_W^{J/\psi}$ (solid curve). Data are from S. Katsanevas et al., Phys. Rev. Lett. **60** (1988) 2121 for J/ψ and from K. Freudenreich. XIII Intern. Conf. on Hight energy physics (Berkeley, July 1986) for DY.

Initial State Effects on J/ψ at RHIC

More low-x:

- Inclusion of the evolution effects.

  M. Nardi et al., Nucl. Phys. **A 855** (2011) 392

  - It was also included the resctriction of a odd number of gluons bound to pair $c\bar{c}$.
  - It is considered that the transformation properties of the $c\bar{c}$ pair are the same as those of J/ψ.
  - The results for model in collisions pA and AA are compared with the data throught of nuclear modification factor

$$R_{AB}(b) = \left(\frac{dN^{AB}}{dy}(b)\right) / \left(N_{coll}(b)\frac{dN^{pp}}{dy}\right)$$

Initial State Effects on J/ψ at RHIC

- Differences pA x AA:

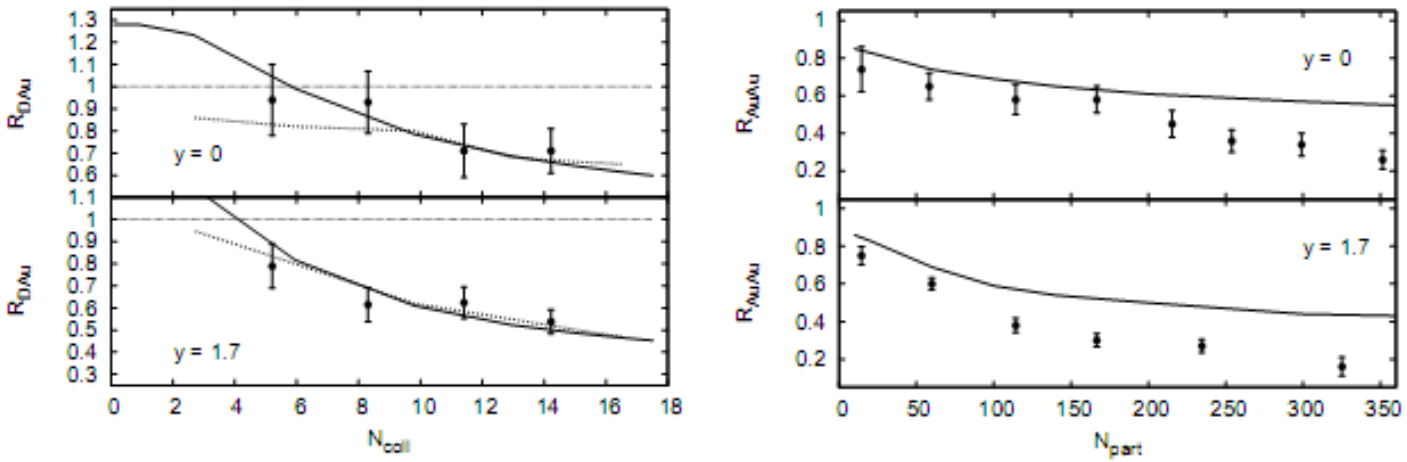

Left: Nuclear modification factor of J/ψ production in d+Au collisions. The solid lines are the results obtained with the "traditional" approach. The dashed lines are the results this new model. Right: Nuclear modification factor of J/ψ production in Au+Au collisions.

Initial State Effects on J/ψ

- Differences pA x AA:
  - The initial state effects mechanism are different for pA and AA collisions.

    B.Z.Kopeliovich, I.K. Potashnikova, and I. Schmidt, EPJ Web Conf. **70** (2014) 00067
  - In collisions AA, the target interacted with other nucleons in the beam nucleus.
  - Such excited nucleons should be accompanied by radiated gluons, where the average number per nucleon is:

$$< n_g >= \frac{3}{\sigma_{inel}(NN)} \int_{k^2_{min}}^{\infty} dk^2 \int_{x_{min}}^{1} dx \frac{d\sigma(qN \to gX)}{d\alpha dk^2} \Theta(\Delta z - l_f^g) = \begin{cases} 6.9\times10^{-1} & (\sqrt{s} = 20 \text{ GeV}) \\ 6.9\times10^{-3} & (\sqrt{s} = 200 \text{ GeV}) \\ 1.2\times10^{-3} & (\sqrt{s} = 1200 \text{ GeV}) \end{cases}$$

$l_f^g = 2E_q x\,(1-x)\,/\,(x^2 m_q^2 + k^2)$ $\rightarrow$ time scale for gluon radiation.

x $\rightarrow$ fractional momentum of the radiated gluon.

Initial State Effects on J/ψ

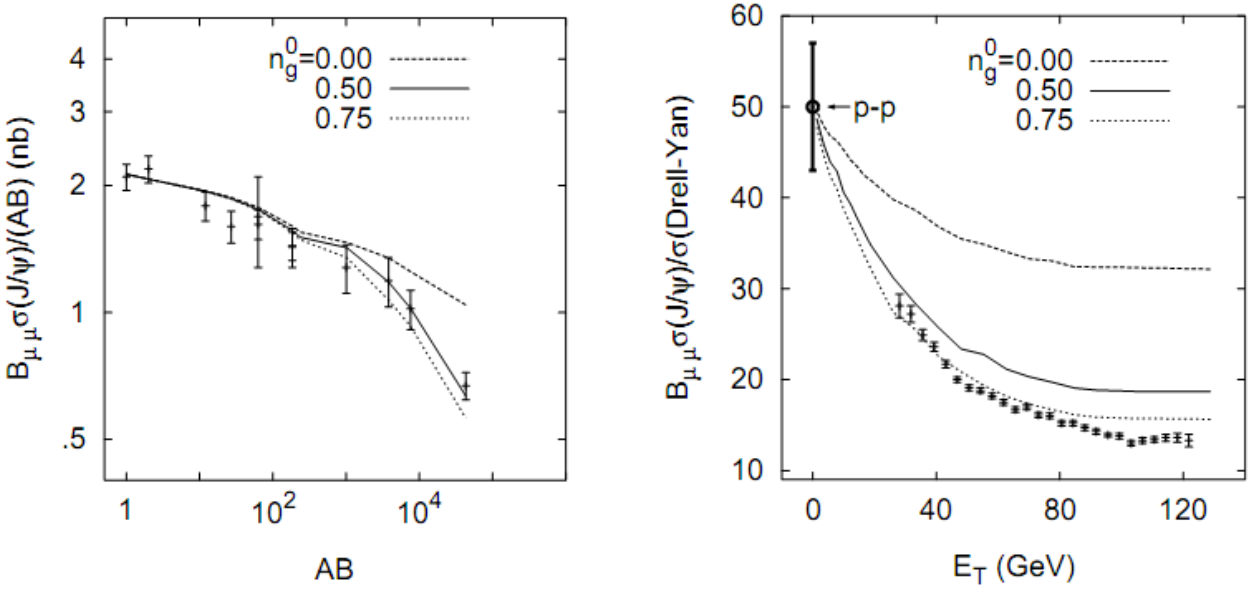

Right: Ratio of J/ψ to Drell-Yan cross section as a function of centrality in S-U collisions at 200 GeV/c, with $< n_g >= 0$, 0.5, 0.75. The calculated curves are normalized at $E_T = 0$ to the ratio observed for p-p collisions. Left: The J/ψ total cross section as a functions of the product AB of the projectile and target atomic mass numbers at 200 GeV/c, for $\langle n_g \rangle = 0$, 0.5, 0.75. All data are from M.C. Abreu et al, Phys. Lett. **B 449** (1999) 128; **B 410** (1997) 337

J/ψ Suppression

- J/ψ suppression can be expected due to several effects:
  - Nuclear absorption.
  - Debye screening in QGP.
  - Saturation effects.
  - Comover Interactions.
  - Percolation deconfinement.
  - ...

J/ψ Suppression in QGP

- Ressonances $c\bar{c}$ (J/ψ, ψ',...) and $b\bar{b} \rightarrow$ shorter radius.
  - It will be required higher temperatures (as in QGP) to dissociate these states.
  - $Q\bar{Q} \rightarrow$ to the plasma $\rightarrow$ binding potential in nuclear medium $\rightarrow$ dissociation of pairs $\rightarrow$ suppression.
  - This, in turn, can be detected experimentally by dileptonic decay mode of J/ψ.
  - The ALICE's dimuon spectrometer is dedicated to look for this type of signal.

Evolution of the Parton Density

- DGLAP $\left(s \approx Q^2 \rightarrow \Sigma \left(\alpha_s \ln Q^2\right)^n \Rightarrow \ln s Q^2\right)$
- BFKL $\left(s \gg Q^2 \rightarrow \Sigma \left(\alpha_s \ln s\right)^n \Rightarrow \ln \left(\frac{s}{x}\right)^2\right)$
- Low energy $\rightarrow$ Valence quarks.
- Increasing energy $\rightarrow$ Sea quarks.
- New partons are emitted.
- DGLAP and BFKL (only emission diagrams).

Saturation of gluon density

- F_2 data increases at small x $\rightarrow$ suggests *violation of unitarity*
- The unitarity limit is the Froissart limit: $\sigma \leq$ cte $\ln^2 s$
- DGLAP and BFKL need a control.
- Possibilities:
  - NLO? $\rightarrow$ Reggeized gluon.
  - Increase in $s \rightarrow$ gluons along ladder $\rightarrow$ low momentum $\sim \Lambda_{\rm QCD}$.
  - pQCD is not consistent at high energy without non-linear terms.

Saturation of gluon density

Increasing Q^2

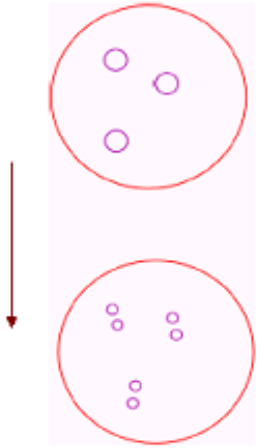

The phase space density decreases.

The proton is diluted.

Decreasing x

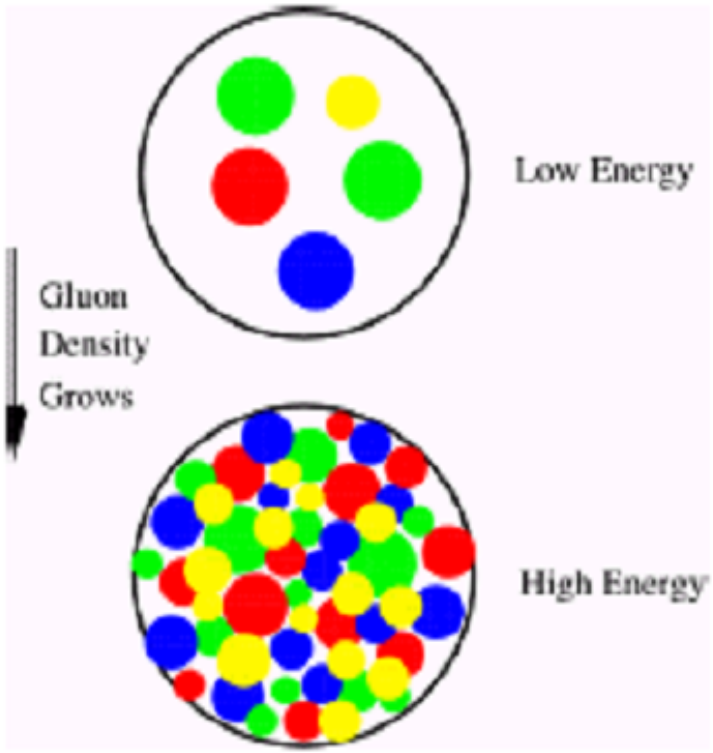

Phase space grows rapidly.

Saturation of gluon density

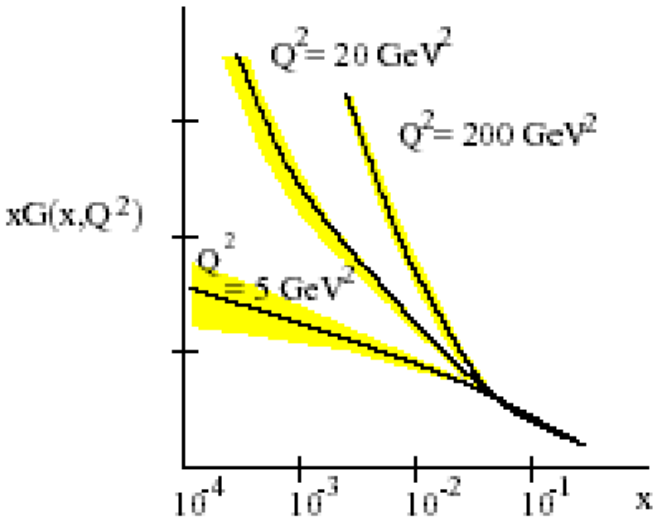

Gluon density grows at small x.

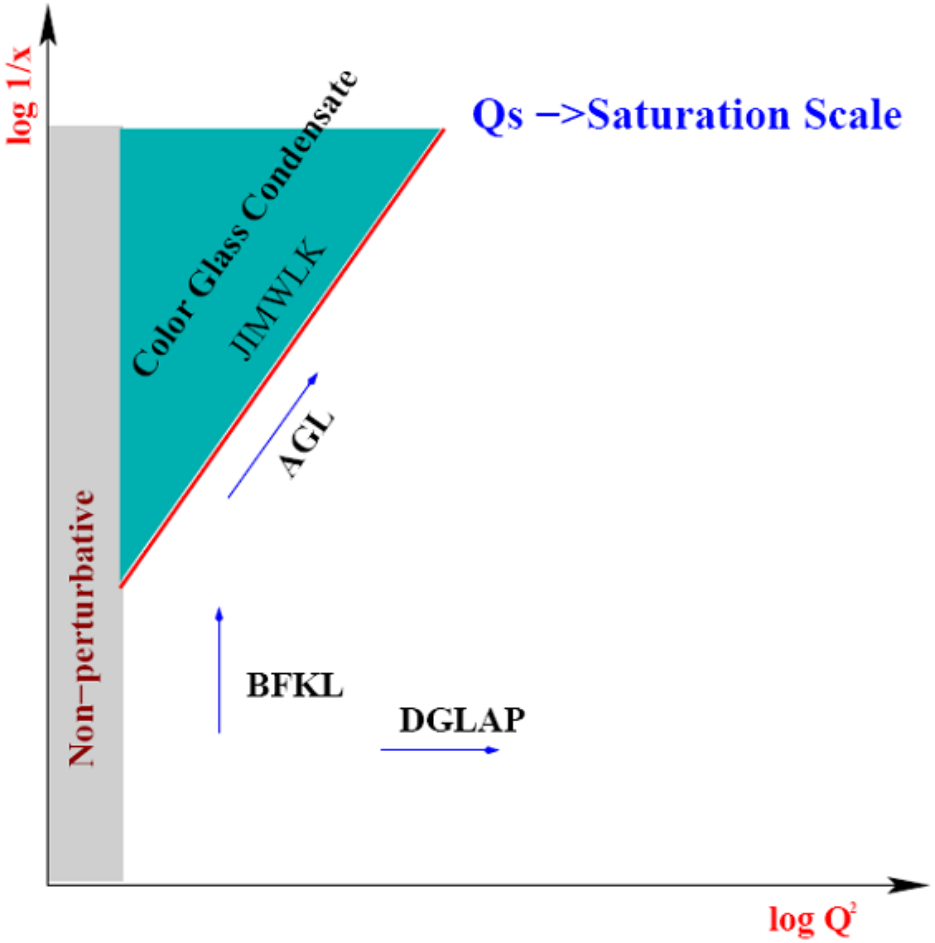

QCD dynamics.

Partonic System Evolution

- At small x region (high energy limit).
- Density of partons increases.
- Large occupation number (partons eventually overlap).
- Recombination process (GLR, AGL, BK, JIMWLK)

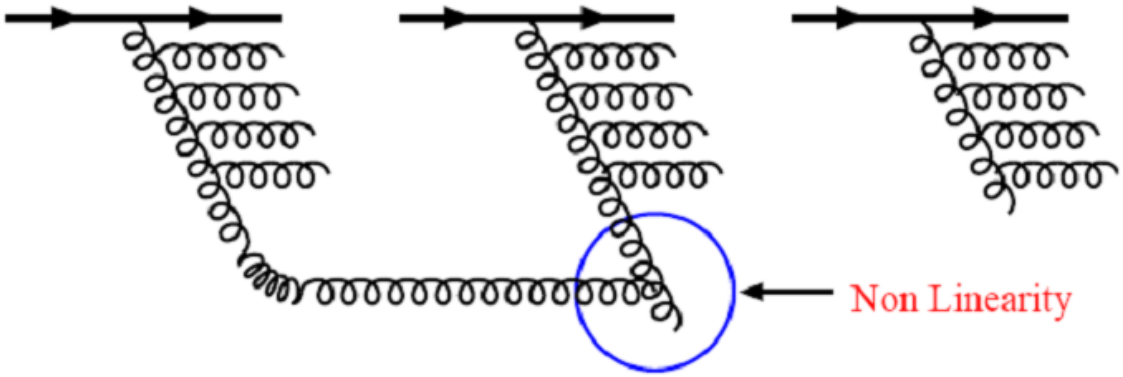

Evolution Equation GLR

$$\frac{\partial^2 xg\left(x,Q^2\right)}{\partial \ln\frac{1}{x}\partial \ln Q^2} = \frac{\alpha_s N_c}{\pi} xg\left(x,Q^2\right) - \frac{81}{16}\frac{\alpha_s^2\left(Q^2\right)}{Q^2}\left[xg\left(x,Q^2\right)\right]^2$$

L.V. Gribov, E.M. Levin and M.G. Ryskin, Phys. Rep. **100** (1983) 1

A.H. Mueller, J. Qiu., Nucl. Phys. **B 268** (1986) 427.

- Mueller and Qiu (1986): $\frac{\bar{\gamma}}{\pi} = \frac{81}{16}$
- Gluon recombination effect: $gg \to g$

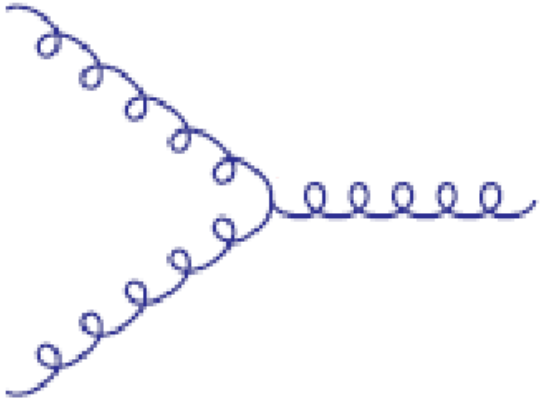

Evolution Equation AGL

- Sum all screening corrections.

$$\frac{\partial^2 xG\left(x,Q^2\right)}{\partial \ln Q^2 \partial \ln\left(\frac{1}{x}\right)} = \frac{2Q^2}{\pi^2}\int db_t^2 \left\{1 - e^{-\frac{1}{2}\sigma\left(x,r_t^2\right)S\left(b_t^2\right)}\right\}$$

A.L. Ayala, M.B. Gay Ducati, E.M. Levin., Phys. Lett. **B 388** (1996) 188.

A.L. Ayala, M.B. Gay Ducati, E.M. Levin., Nucl. Phys. **B 493** (1997) 305.

A.L. Ayala, M.B. Gay Ducati, E.M. Levin., Nucl. Phys. **B 511** (1998) 355.

- Small distances $\rightarrow$ theoretically known.
- Large distances $\rightarrow$ non-perturbative effects $\rightarrow$ boundary and initial conditions.
- Generalized evolution equation.
- Interaction of all partons in a parton cascade.

Evolution Equation AGL

- Solving asymptotic equation:
  - A dependence.
  - Increase of non-linear effects.
  - Onset of saturation.

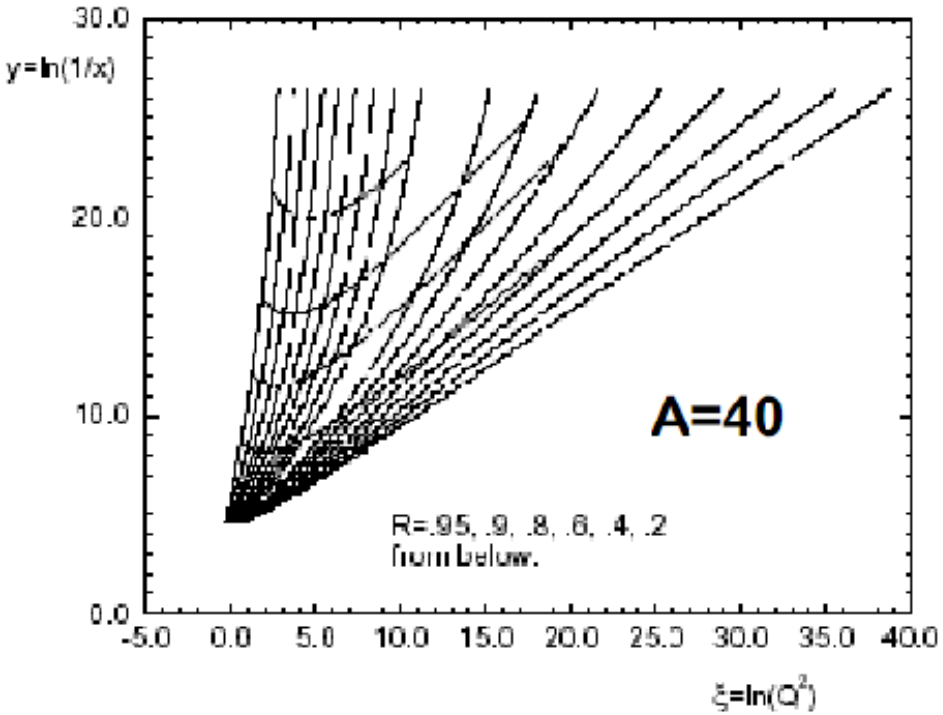

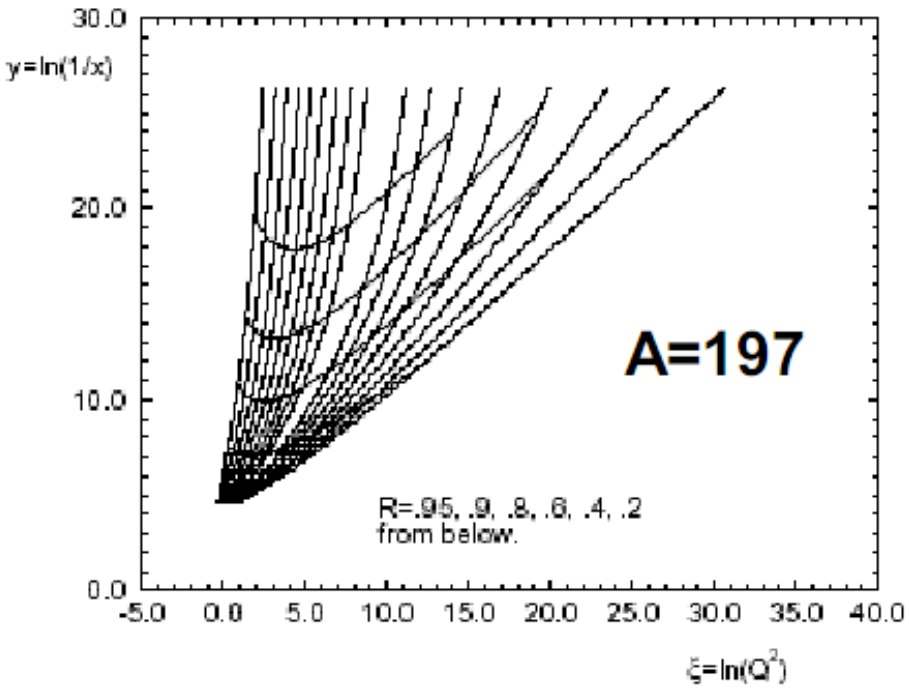

Linear Equations

- **Linear evolution**
  - DGLAP ($\sim$1977) evolves quark and gluon distributions in Q^2.

$$\frac{dg(x,Q^2)}{d\ln Q^2} = \frac{\alpha_s(Q^2)}{2\pi}\int_x^1 \frac{dy}{y}\left[P_{gq}\left(\frac{x}{y}\right) q_i^S\left(y,Q^2\right) + P_{gg}\left(\frac{x}{y}\right) g\left(y,Q^2\right)\right]$$

  - BFKL ($\sim$1977) evolves non-integrated gluon distribution in x.

$$\frac{\partial\phi(x,k_\perp^2)}{d\ln(1/x)} = \frac{3\alpha_s}{\pi}k_\perp^2\int_0^\infty \frac{dk_\perp'^2}{dk_\perp'^2}\left\{\frac{\phi\left(x,k_\perp'^2\right)+\phi\left(x,k_\perp^2\right)}{\left|k_\perp'^2-k_\perp^2\right|} + \frac{\phi\left(x,k_\perp^2\right)}{\sqrt{4k_\perp'^4+k^4}}\right\}$$

Non-Linear Equations

- **Non-linear evolution**
  - GLR (1983) evolves $xg(x, Q^2)$ in x and Q^2.

$$\frac{\partial^2 xg\left(x,Q^2\right)}{\partial \ln Q^2 \partial \ln 1/x} = \frac{\alpha_s N_c}{\pi} xg\left(x, Q^2\right) - \frac{\alpha_s^2 \gamma}{Q^2 R^2}\left[xg\left(x, Q^2\right)\right]^2$$

  - AGL (1997) evolves $\kappa_G(x, Q^2) = \frac{N_c \alpha_s \pi}{2 Q^2 R^2} xg(x, Q^2)$ in x and Q^2.

$$\frac{\partial^2 \kappa_G\left(x,Q^2\right)}{\partial(\ln 1/x)\partial(\ln Q^2)} + \frac{\partial \kappa_G\left(x,Q^2\right)}{\partial(\ln 1/x)} = \frac{N_c \alpha_s}{\pi}\left[C + \ln\left(\kappa_G\right) + E_1\left(\kappa_G\right)\right]$$

  - BK (1996-1999) evolves the dipole density (N) in $Y = \ln(1/x)$.

$$\frac{\partial^2 N\left(\vec{x}_{01},\vec{b}_0,Y\right)}{\partial Y \partial \ln\left(1/x_{01}^2 \Lambda_{QCD}^2\right)} = \frac{\alpha_s C_F}{\pi}\left[2 - N\left(\vec{x}_{01}, \vec{b}_0, Y\right)\right] N\left(\vec{x}_{01}, \vec{b}_0, Y\right)$$

  - JIMWLK ($\sim$1997-01) evolves the color charge sources correlation in $Y = \ln(1/x)$

$$\frac{\partial W_Y[\rho]}{\partial Y} = \frac{1}{2}\int \frac{\delta}{\delta \rho_Y^a(x_\perp)} \chi_{ab}(x_\perp, y_\perp)[\rho] \frac{\delta}{\delta \rho_Y^b(y_\perp)} \mathcal{W}_Y[\rho]$$

Exploring Low-x Physics - Forward Process

- All LHC experiments have the operational capacity to study forward processes.
  - Forward cross sections $\rightarrow$ High energy or density QCD.
  - $\gamma + p \rightarrow V + p \rightarrow$ has been investigated experimentally and theoretically as it allows to test perturbative Quantum Chromodynamics.

- The quarkonium masses(m_c, m_b), give a perturbative scale for the problem even at $Q^2 = 0$

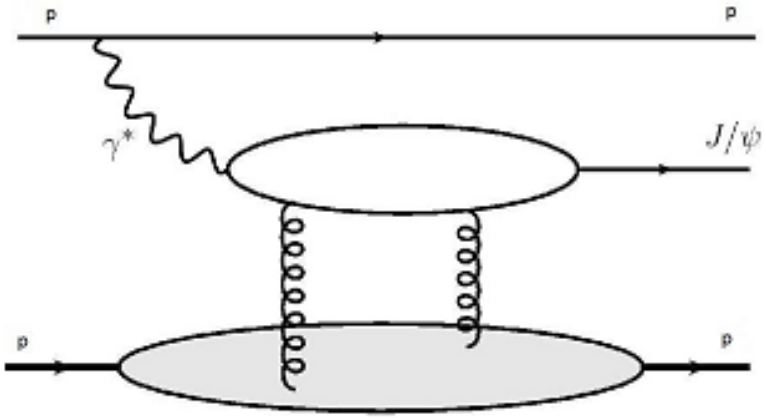

Light cone wave functions

- The light cone wave functions of the meson are written as:

$$\Psi^{V,L}_{h,\bar{h}}(r,z) = \sqrt{\frac{N_c}{4\pi}}\delta_{h,-\bar{h}}\frac{1}{M_V z(1-z)}\left\{z(1-z)M_V^2 + \delta\left[m_f^2 - \left((1/r)\partial_r + \partial_r^2\right)\right]\right\}\phi_L(r,z)$$

$$\Psi^{V,T(\gamma=\pm)}_{h,\bar{h}}(r,z) = \pm\sqrt{\frac{N_c}{4\pi}}\frac{\sqrt{2}}{z(1-z)}\{ie^{\pm i\theta_r}[z\delta_{h\pm,\bar{h}\mp} - (1-z)\delta_{h\mp,\bar{h}\pm}]\partial_r + m_f\delta_{h\pm,\bar{h}\mp}\}\phi_T(r,z)$$

- For J/ψ and ψ':

J. R. Forshaw, R. Sandapen and G. Shaw, JHEP 0611, 025, 2006

$$\phi_\lambda(r,z) = N_\lambda\left[4z(1-z)\sqrt{2\pi R^2}\exp\left(-\frac{m_f^2R^2}{8z(1-z)}\right)\exp\left(-\frac{2z(1-z)r^2}{R^2}\right)exp\left(\frac{m_f^2R^2}{2}\right)\right]$$

$$\phi_{2S}(r,z) = \phi_{1S}(r,z)\left[1 + \alpha_{2S}\left(2 - m_f^2R_{2S}^2 + \frac{m_f^2R_{2S}^2}{4z(1-z)} - \frac{4z(1-z)r^2}{R_{2S}^2}\right)\right]$$

J. Nemchik, N. N. Nikolaev, E. Predazzi and B. G. Zakharov, Phys. Lett. **B 374** (1996) 199

GBW and CGC Dipole Cross Section

- The GBW (Golec-Biernat and Wusthoff) parametrization:

K. Golec-Biernat and M. Wusthoff, Phys. Rev. **D 59** (1999) 014017

$$\sigma_{dip}(x,\vec{r};\gamma) = \sigma_0 \left[1 - \exp\left(-\frac{r^2 Q_{sat}^2}{4}\right)^{\gamma_{\rm eff}}\right],$$

  - $\gamma_{\rm eff} = 1$; Saturation scale $\rightarrow Q_{sat}^2(x) = \left(\frac{x_0}{x}\right)^{\lambda}$
  - x_0, σ_0, $\lambda \rightarrow$ fitted to DIS HERA data

- The Color Glass Condensate (CGC) paremetrization:

E. Iancu, K. Itakura and S. Munier, Phys. Lett. **B 590** (2004) 199

$$\sigma_{dip} = \begin{cases} 2\pi R^2 N_0 \left(\frac{rQ_s}{2}\right)^{2\{\gamma_s + [\ln(2/rQ_s)/\kappa\lambda \ln(1/x)]\}} & ,rQ_s \leq 2 \\ 2\pi R^2 \{1 - \exp\left[-a \ln^2(brQ_s)\right]\} & ,rQ_s > 2 \end{cases}$$

  - $Q_s = (x_0/x)^{\lambda/2} GeV \rightarrow$ saturation scale
  - $\gamma_s = 0.63$, $\kappa = 9.9 \rightarrow$ fixed to their LO BFKL values
  - R, x_0, $\lambda \rightarrow$ free parameters of the fit

Cross Section and Ratios

Total cross section for forward region:

- Our prediction

$$\sigma_{pp\to\psi(2S)(\to\mu^+\mu^-)}(2.0 < \eta_{\mu^\pm} < 4.5) = 7.7 \text{ pb}$$

- LHCb measure, R Aaij et al, J. Phys. G: Nucl. Part. Phys. **40** (2013) 04500

$$\sigma_{pp\to\psi(2S)(\to\mu^+\mu^-)}(2.0 < \eta_{\mu^\pm} < 4.5) = 7.8 \pm 1.6 \text{ pb}$$

Ratio $\Psi(2S)/\Psi(1S)$ ratio:

- Our prediction

$$[\psi(2S)/\psi(1S)]_{y=0} = 0.16$$
$$[\psi(2S)/\psi(1S)]_{2<y<4.5} = 0.18$$

- LHCb determination, R Aaij et al, J. Phys. G: Nucl. Part. Phys. **40** (2013) 04500

$$[\psi(2S)/\psi(1S)](2.0 < \eta_{\mu^\pm} < 4.5) = 0.19 \pm 0.04$$

J/Ψ and Ψ' production in AA collisions

- Coherent process: $AA \to AA + J/\Psi(\Psi')$.
  - Nuclei remain intact.
  - Cross section: B. Z. Kopeliovich and B. G. Zakharov, Phys. Rev. D 44, 3466, 1991

$$\sigma^{cohe}(\gamma A \to J/\Psi A) = \int d^2b \left\{ \left| \int d^2r \int dz \Psi_V^*(r,z) \left(1 - \exp\left[-\frac{1}{2}\sigma_{dip}(x,r)\, T_A(b)\right]\right) \Psi_{\gamma^*}(r,z,Q^2) \right| \right\}$$

$T_A(b) = \int dz \rho_A(b,z)$

$\rho_A(b,z) \to$ nuclear thickness function.

- Incoherent process: $AA \to AA^* + J/\Psi(\Psi')$.
  - One nuclei is excited.
  - Cross section:

$$\sigma^{inc}(\gamma A \to J/\Psi X) = \frac{1}{16\pi B_V} \int d^2b T_A(b) \left[\left| \int d^2r \int dz \Psi_V^*(r,z) \sigma_{dip} \exp\left[-\frac{1}{2}\sigma_{dip} T_A(b)\right] \Psi_{\gamma^*}(r,z,Q^2) \right|^2 \right]$$

with $B_V = 0.6 \times \left(\frac{14}{(Q^2+M_V^2)^{0.26}} + 1 \right) \to$ diffractive slope parameter, $\gamma^* p \to \Psi p$

$\Psi(1S)$ and $\Psi(2S)$ rapidity distribution

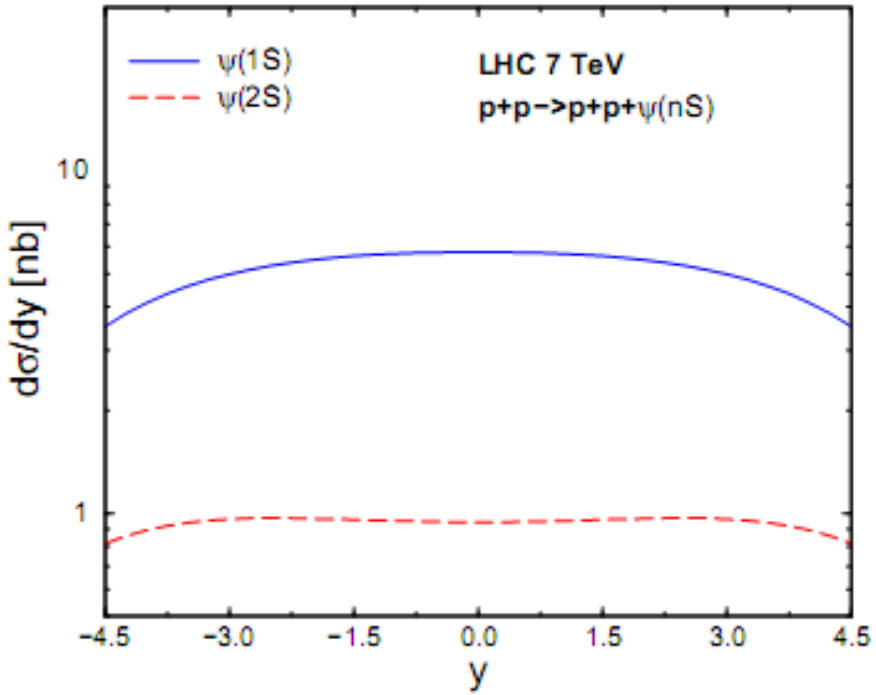

The rapidity distribution of $\Psi(1S)$ and $\Psi(2S)$ photoproduction at $\sqrt{s} = 7\,TeV$ *

- Predictions to LHC $7\,TeV$, pp, including mid-rapidity and backward regions;
- The model CGC was considered for the dipole cross section;
- $\Psi(1S) \rightarrow y = 0$: $d\sigma/dy \approx 5.8nb$;
- $\Psi(2S) \rightarrow y = 0$: $d\sigma/dy \approx 0.94nb$.

M. B. Gay Ducati, M. T. Griep and M. V. T. Machado, Phys. Rev. **D 88** (2013) 017504

Comparison with LHCb data

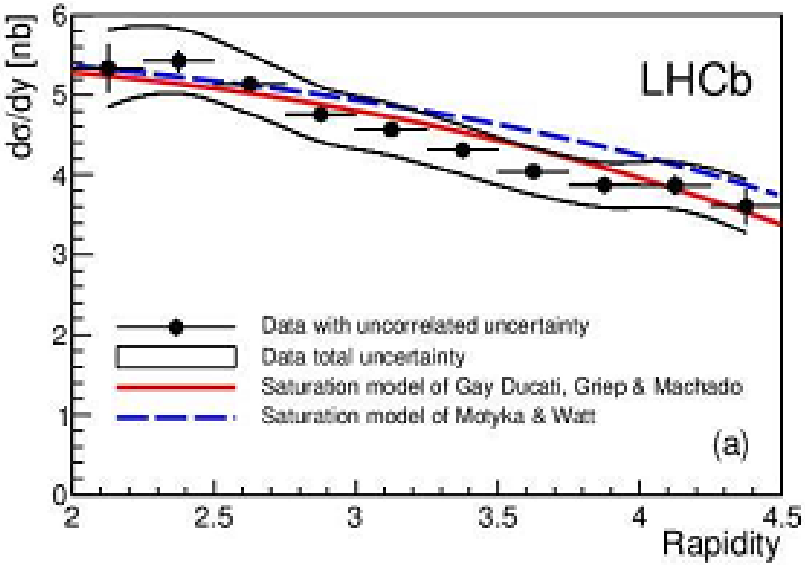

Rapidity distribution of J/Ψ

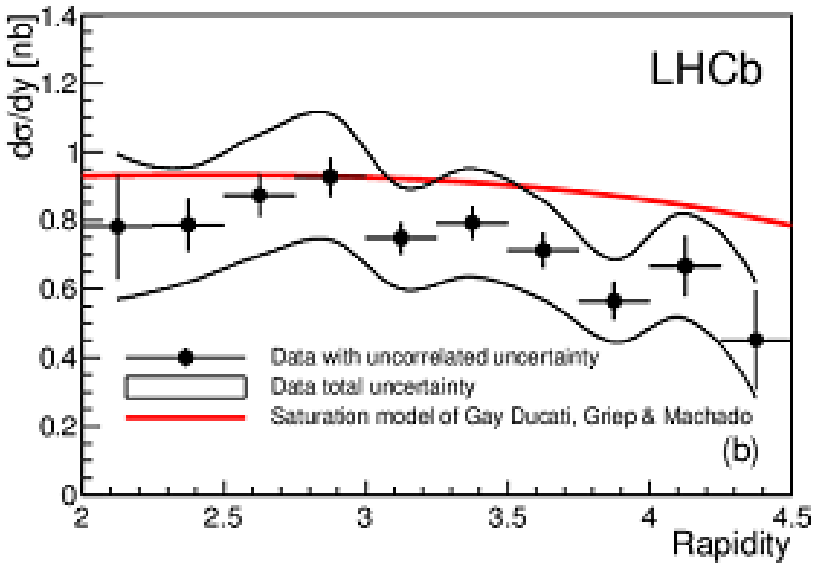

Rapidity distribution of $\Psi(2S)$.

$\Rightarrow$ Good agreement with the data is observed

The LHCb Collaboration; AAIJ, R., Nucl. Part. Phys. 41, 055002, 2014.

Differential cross section for Υ production.

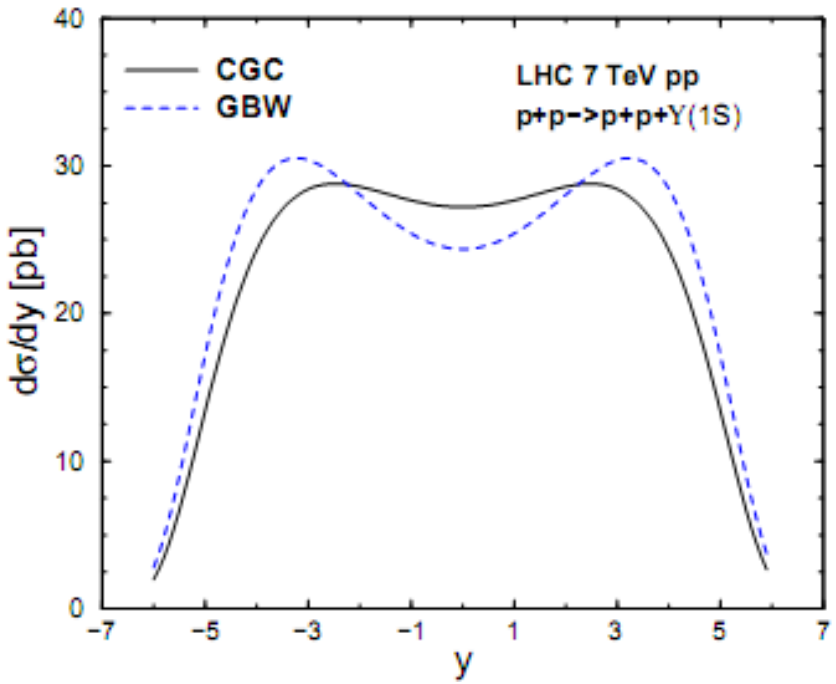

The rapidity distribution of Υ photoproduction at $\sqrt{s} = 7\,TeV$.

- Predictions for LHC $7\,TeV$, pp ;
- The models CGC and GBW were considered for the dipole cross section;
- Work in progress.

Differential cross section for J/Ψ production

- R_G Model 1 $\rightarrow$ higher nuclear shadowing $\rightarrow$ Pomeron - 2 gluons.
- R_G Model 2 $\rightarrow$ small nuclear shadowing $\rightarrow$ Pomeron soft.

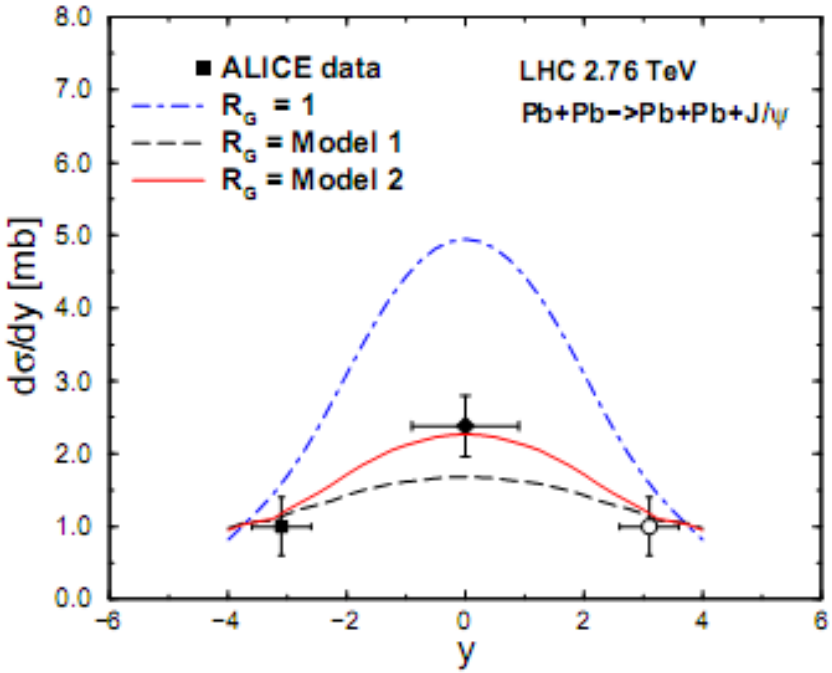

The rapidity distribution of coherent $\Psi(1S)$ meson photoproduction at $\sqrt{s} = 2.76$ TeV in PbPb collisions at the LHC

- $\sigma_{dip} \rightarrow R_G(x, Q^2)\sigma_{dip}$;
- $R_G = 1$: the ALICE data is overestimate by a factor 2;

  V. P. Goncalves and M. V. T. Machado, Phys. Rev. **C 84** (2011) 011902;
- In the backward/forward rapidity case, the overestimation is already expected as a proper threshold factor for $x \rightarrow 1$ was not included in the present calculation.
- R_G Model 2 is preferred in this analysis.

  ALICE data: Phys. Lett. **B 718** (2013) 1273

M. B. Gay Ducati, M. T. Griep and M. V. T. Machado, Phys. Rev. **C 88** (2013) 014910

Differential cross section for Ψ' production

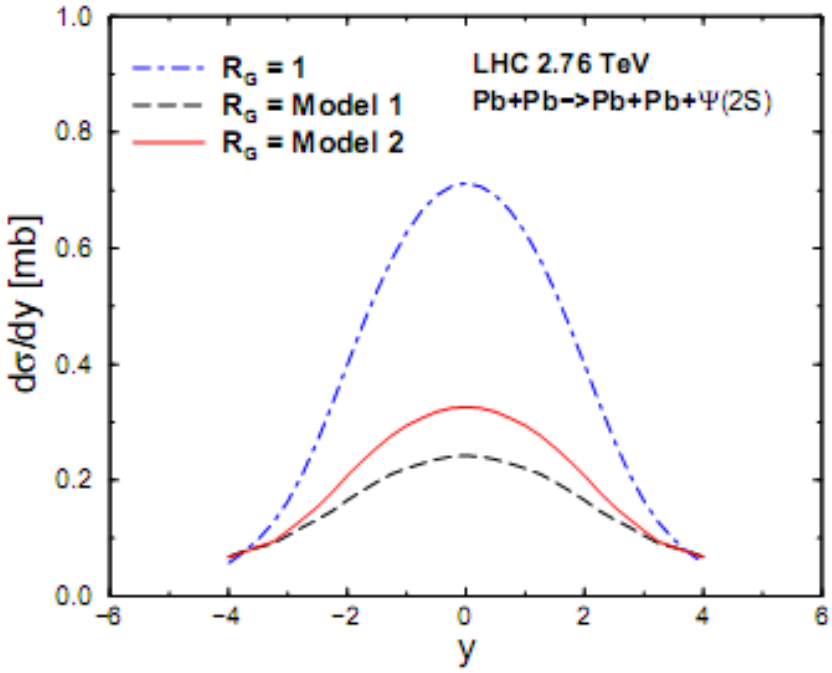

The rapidity distribution of coherent $\Psi(2S)$ meson photoproduction at $\sqrt{s} = 2.76$ TeV in PbPb collisions at the LHC

- The theoretical curves follow the same notation as in the $\Psi(1S)$ case;

M. B. Gay Ducati, M. T. Griep and M. V. T. Machado, Phys. Rev. **C 88** (2013) 014910

Analyzing the ratio $\Psi(2S)/\Psi(1S)$

- At central rapidities, the presented predictions give the ratio

$$R_{\psi}^{y=0} = \frac{d\sigma_{\psi(2S)}}{dy} / \frac{d\sigma_{\psi(1S)}}{dy}(y=0) = 0.14$$

- To $R_G = 1 \rightarrow$ consistent with the ratio measured in CDF: 0.14 ± 0.05 (exclusive charmonium production at 1.96 TeV in $p\bar{p}$ collisions)

  T. Aaltonen et al (CDF Collaboration), Phys. Rev. Lett. 102, 242001 (2009)

- A similar ratio is obtained using Model 1 and Model 2 at central rapidity.
- the ratio is not sensitive to shadowing.

Differential cross section for incoherent J/Ψ and Ψ' production.

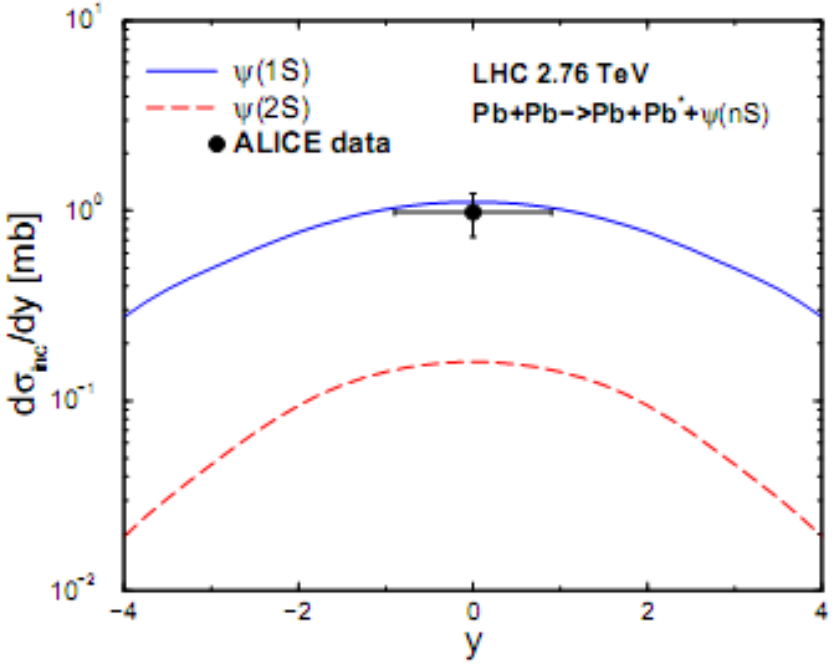

- Data from ALICE collaboration;
- The result describes the recent ALICE data for the incoherent cross section at mid-rapidity;
- In both cases we only computed the case for $R_G = 1$;

ALICE data: Eur. Phys. J.C (2013) 73: 2617.

The rapidity distribution of incoherent $\Psi(1S)$ (solid line) and $\Psi(2S)$ (dashed line) meson photoproduction at $\sqrt{s} = 2.76$ TeV in PbPb collisions at the LHC,
M. B. Gay Ducati, M. T. Griep and M. V. T. Machado, Phys. Rev. **C 88** (2013) 014910

Results

- $\Psi(1S)$ $\rightarrow$ the prediction describes the recent ALICE data.

$$\frac{d\sigma_{\rm inc}}{dy}(y=0) = 1.1\ mb$$
$$\frac{d\sigma_{inc}^{\rm ALICE}}{dy}(-0.9 < y < 0.9) = 0.98 \pm 0.25\ mb$$

- $\Psi(2S)$ $\rightarrow$ For the incoherent case, the gluon shadowing is weaker than the coherent case - 20% reduction compared to $R_G = 1$.

$$\frac{d\sigma_{\rm inc}}{dy} = 0.16\ mb$$

- Prediction for the LHC run in PbPb mode at 5.5 TeV with $R_G = 1$:
  - **Coherent**$\rightarrow$ $\frac{d\sigma_{coh}}{dy}(y=0) = 1.27\ mb$.
  - **Incoherent**$\rightarrow$ $\frac{d\sigma_{inc}}{dy}(y=0) = 0.27\ mb$.

Comparison with ALICE preliminary data

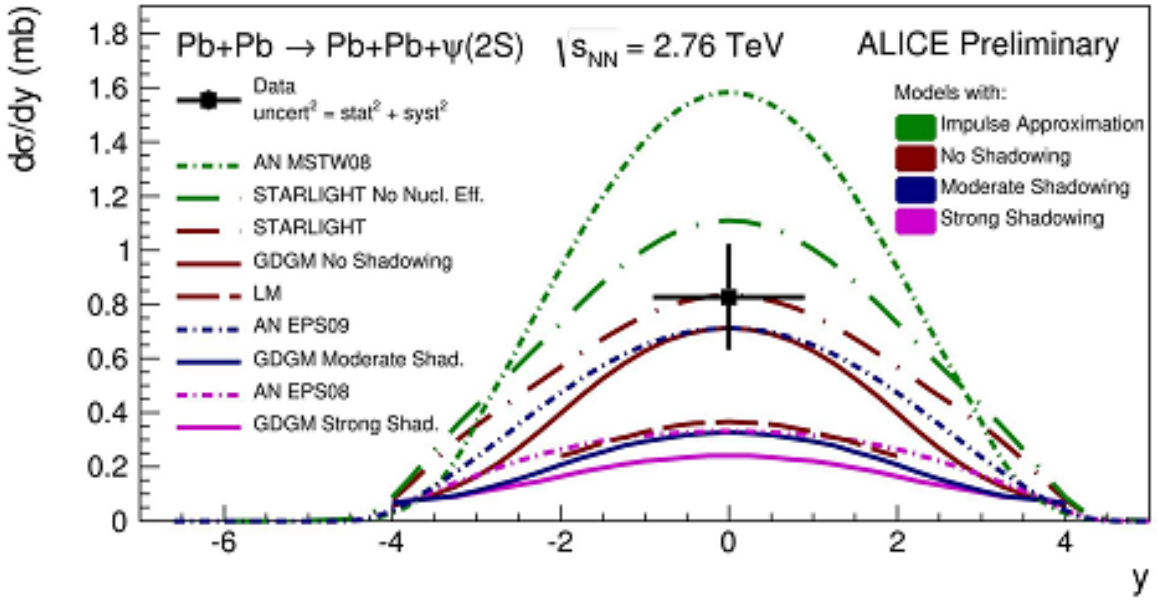

The rapidity distribution of $\Psi(2S)$ photoproduction at $\sqrt{s} = 2.76\,TeV$ compared to ALICE preliminary data.

Michal Broz - ALICE Collaboration -LHCP 2014

$\Rightarrow$ The experimental and theoretical uncertainties prevent any stronger conclusion from the $\Psi(2S)$ measurement at the moment

R_{pA} Forward rapidity and p_T

- Lepton pair mass M=6 GeV
- Suppression at small p_T
- Suppression of the Cronin peak;
- RHIC $\sqrt{s} = 200$ GeV
  - Small effects in the rapidity spectra;
  - Effects are independent of the p_T value;
- LHC $\sqrt{s} = 8.8$ TeV
  - Suppression in the rapidity spectra is intensified for large p_T
  - Similar behavior of the ratio in p_T at M=3 GeV.

M.A.Betemps, MBGD, Phys. Lett. B, **636**, (2006) 46

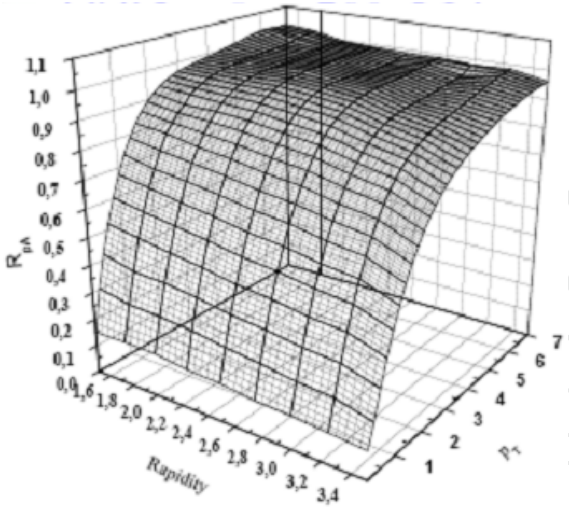

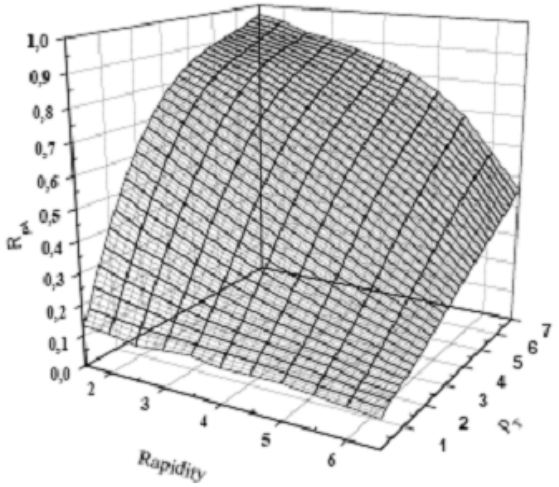

Comparing RHIC and LHC

- Comparing saturation effects at RHIC and LHC.
- Defining the ratio: Ratio $= \dfrac{R_{pA}(LHC)}{R_{pA}(RHIC)}$.

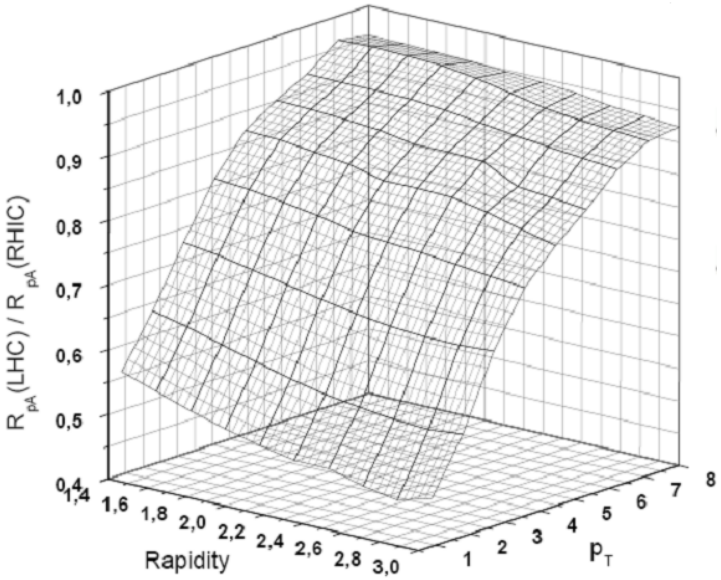

- Small saturation effects in rapidity comparing RHIC and LHC (RHIC range only)
- Large saturation effects at LHC comparing with RHIC in the p_T distribution.

Next

Inspired in F. Antinori et al, Hep-ph/1409.2981

Initial State

- Wave functions of hadrons and nuclei $\rightarrow$ constructing equilibration in QCD.
  - Gluons at initial state are weakly or strongly coupled?
  - Holographic methods to map dynamics can be connected to experimental measurements?
  - Formulation of Multiple Partonic Interactions (MPI)
  - Comparison eA x pA for dynamics of partons in cold nuclear matter.

Initial Conditions

- Event-by-event IC fluctuations $\rightarrow$ small nuclei collisions.
- Soft Physics observables $\rightarrow$ anisotropic flows.
- Magnetic fields and vorticity (RHIC)
  (Chiral magnetohidrodynamics)

Next

Jets + Heavy Flavors

- Properties of QGP at different lenght scales
- Multiparticle correlations.
- High heavy quarks productions $\rightarrow$ colour-charged dependence of energy loss - $q \times g$.
- Weakly coupled approaches $\times(+)$ strong parton medium coupling.
- Reconstruction of jet measurements.
- Next generation MC (NLO).

Next

Hadronization

- Lattice transition $qg \rightarrow$ hadronic matter.
- Freezout dynamics.
- Fluctuations x system size (d,A,...)
- Charmonium suppression $\rightarrow$ SPS(RHIC) X LHC
- Statistical recombination $\rightarrow$ hadronization of thermalized charm quarks.
- Bottomonium x charmonium at LHC $\rightarrow p_T$ dependence.

+ phase diagram:

- From SPS to LHC
- Collective behavior
- ...